Theoretical investigation on the presence of different iron sites in RbMn[Fe(CN)6]·H2O

Kurian, Reshmi; Filatov, Michael

Published in:
Journal of Physics: Conference Series

DOI:
10.1088/1742-6596/217/1/012012

Publication date:
2010

Journal of Physics: Conference Series **217** (2010) 012012 doi:10.1088/1742-6596/217/1/012012

Theoretical investigation on the presence of different iron sites in $RbMn[Fe(CN)_6]\cdot H_2O$

Reshmi Kurian and Michael Filatov

Theoretical Chemistry, Zernike Institute for Advanced Materials,Rijksuniversiteit Groningen,Nijenborgh 4, 9747 AG Groningen, The Netherlands

E-mail: m.filatov@rug.nl

Abstract. The ^{57}Fe electron contact densities and the corresponding Mössbauer isomer shifts of $RbMn[Fe(CN)_6]\cdot H_2O$ are calculated with the use of *ab initio* wavefunction methods and double hybrid density functional method. The theoretical analysis of possible origin of the two slightly different signals in the Mössbauer spectra observed at 293 K and 50 K (Vertelman *et al.* 2008 *Chem. Mater.* **20** 1236-38) is carried out. The measured differences of 0.083 - 0.105 mm/s between the high-temperature and low-temperature phases can be attributed to the different oxidation states of iron: the iron is in Fe^{III} oxidation state in the high temperature phase and Fe^{II} state in the low temperature phase. The smaller isomer shift differences of 0.012 - 0.034 mm/s occurring in both high temperature and low temperature structures can be attributed to different distributions of the Rb^{I} ions within the unit cell of $RbMn[Fe(CN)_6]\cdot H_2O$.

1. Introduction

In the present work, theoretical analysis of ^{57}Fe Mössbauer isomer shifts in a Prussian blue analogue $RbMn[Fe(CN)_6]\cdot H_2O$ is carried out. Prussian blue analogues are compounds with the general molecular formula $A_xM^a[M^b(CN)_6]\cdot zH_2O$ (where, A = alkali cation and M^a/M^b = metal ion), which attract considerable interest due to their peculiar magneto-optical properties [1]. Thus, $RbMn[Fe(CN)_6]\cdot H_2O$ shows light and temperature induced switching of magnetization [2]. Upon cooling from 300K to approximately 150K, $RbMn[Fe(CN)_6]\cdot H_2O$ undergoes transition to a state with higher molar magnetization. A reversed transition to a low magnetization state is observed upon heating to *ca.* 250K. It has been hypothesized that the switching of magnetization occurs due to electron transfer from the Mn^{II} cations to the Fe^{III} ions (and reversed transition) as a result of structural phase transition upon cooling/heating the samples [3].

The Mössbauer spectra of the high-temperature (HT) and the low-temperature (LT) structures

Table 1. ^{57}Fe Mössbauer isomer shifts observed in $RbMn[Fe(CN)_6]\cdot H_2O$ at different temperatures [3] where number in the parentheses shows the experimental uncertainty in the last digit .

T, K	δ, mm/s	
50	-0.033(4)	-0.067(5)
293	-0.138(2)	-0.150(2)

were recorded whereby it was observed that, in both structures, two signals with the isomer shifts reported in Table 1 were present [3]. The presence of two different Fe^{III} sites in the HT phase of

$RbMn[Fe(CN)_6]\cdot H_2O$ with the shifts $\delta = -0.138(2)$ mm/s and $\delta = -0.150(2)$ mm/s was interpreted as a consequence of different distributions of the Rb cations over the interstitial sites 4*c* and 4*d* (see Figure 1) in the space group $F\bar{4}3m$ of the crystal. Although it was not possible to obtain reliable crystal structures of the LT phase of $RbMn[Fe(CN)_6]\cdot H_2O$, it is clear that iron is present in the form of low-spin Fe^{II} ions octahedrally coordinated by the cyano ligands. Similar to the HT phase, a disorder in the occupation of the Rb sites around the Fe^{II} ions leads to emergence of two different iron sites as can be seen from the isomer shifts reported in Table 1.

To obtain insight into the origin of different iron sites in the HT and LT structures of

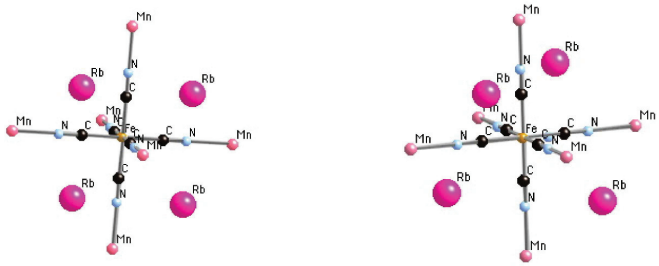

Figure 1. Two different iron sites in $RbMn[Fe(CN)_6]\cdot H_2O$ originating from different distribution of the Rb ions, the cluster shown first is referred as Type I and second as Type II respectively [3].

$RbMn[Fe(CN)_6]\cdot H_2O$ we undertake quantum chemical calculations of ^{57}Fe Mössbauer isomer shifts in cluster models of these sites. More specifically, our goal is to elucidate whether the observed isomer shifts originate from variations in the oxidation state of iron ions (Fe^{II} *vs.* Fe^{III} isomer shifts) and from differences in the coordination sphere of iron ions due to different distribution of the Rb^{I} ions (see Figure 1).

2. Details of calculations

The calculations are carried out in the embedded cluster approach, where the geometries of clusters shown in Fig. 1 are obtained from crystal structure of the HT phase reported in Ref. [3]. The iron is in octahedral coordination with six cyano ligands bridging Fe and Mn. The disorder in the distribution of Rb^{I} ions is modeled by selecting two possible distribution patterns of Rb^{I} around iron atoms as shown in Fig. 1. The Fe-C and Mn-N distances are 1.929 Å and 2.205 Å respectively. The same geometry of clusters is used for the LT phase calculations. The Madelung field is modeled by the field of a large array of point charges placed at the appropriate crystallographic positions.

The calculations are carried out using Hartree-Fock (HF), second order Møller-Plesset perturbation theory (MP2) [4], Coupled Cluster Singles and Doubles (CCSD) [4] and double hybrid density functional (B2-PLYP [5]) level. The 24s12p9d basis set of Partridge with a set of polarization functions taken from TZVpp basis set of Ahlrichs and May [6] is used for iron and 6-31G* [7] basis set is used for carbon and nitrogen. All basis sets were used in uncontracted form. The Rb^{I} core is modeled by the Stuttgart effective core potential (ECP) [8], whereas $Mn^{II/III}$ cores are modeled by the representative ECPs of Ca^{II} and Al^{III}, respectively. The closed shell systems are treated with spin restricted formalism and the open-shell systems with spin unrestricted formalism. The relativistic calculations are carried out within the one-electron approximation [9] and using the normalized elimination of the small component (NESC) [10] method which was implemented according to Ref. [11].

The ^{57}Fe isomer shifts are calculated using a formalism in which the isomer shift is treated as a response of the total electronic energy with respect to the variation of the nuclear charge radius [12, 13, 14]. The isomer shift is related to the contact density as $\delta = \alpha(\bar{\rho}_e^a - \bar{\rho}_e^s)$ where the calibration constant $\alpha(^{57}\text{Fe})$ = -0.306 ± 0.009 mm/s is taken from theoretical calibration of ^{57}Fe isomer shift [15] and $\bar{\rho}$ is obtained from Eq. (1).

$$\bar{\rho}_e^{a/s} = \frac{5}{4\pi Z R}\frac{\delta E_e^{a/s}}{\delta R} \tag{1}$$

The derivatives $\delta E_e(R)/\delta R$ are calculated numerically using the increment of 10^{-6} Bohr for the root mean square (r.m.s.) nuclear charge radius ($R_{Fe} = 0.70213 \times 10^{-4}$ bohr). Throughout this work, the

Gaussian nucleus model [16] is used in the calculations.

3. Results and Discussion

In this section, the influence of different factors, both electronic and geometric, on the ^{57}Fe contact densities of RbMn[Fe(CN)$_6$]·H$_2$O crystal are presented and discussed in detail. The main goal is to determine the origin of the different Fe sites observed in the HT and LT phases (see Table. 1)[3]. In

Table 2. ^{57}Fe electron contact densities and isomer shift differences obtained at different theory levels.

	Fe^{II}	Fe^{III}	$\Delta\rho$	$\Delta\delta$
HF	14938.17	14940.12	-1.95	0.60
MP2	14940.16	14939.82	0.35	-0.11
B2-PLYP	15140.18	15140.89	-0.71	0.22
CCSD	14940.38	14940.70	-0.52	0.16

RbMn[Fe(CN)$_6$]·H$_2$O, iron can be present either in the Fe^{II} or Fe^{III} oxidation states depending on the charge transfer between iron and manganese. In this work, we have carried out calculations on both oxidation states of iron incorporated in clusters described in the previous section. In both oxidation states, iron is assumed to be present in a low-spin state: spin 0 in Fe^{II} clusters and spin 1/2 in Fe^{III} clusters.

Table 2 gives the ^{57}Fe electron contact densities and isomer shifts obtained at different levels of theory (type I coordination sphere shown in Fig. 1 is assumed in these calculations). From the earlier theoretical works on K$_4$Fe(CN)$_6$ and K$_3$Fe(CN)$_6$, $\Delta\delta$ (Fe^{II} - Fe^{III}) is expected to be positive [18]. The Hartree-Fock, B2-PLYP and CCSD yield positive $\Delta\delta$ values while MP2 yields a negative value (see Table 2). From Table 2, it is obvious that the $\Delta\delta$ values obtained with the use of the methods including electron correlation are in much better agreement with the experimental observations than the HF value ($\Delta\delta_{\mathrm{CCSD}} = 0.16$ mm/s and $\Delta\delta_{\mathrm{B2-PLYP}} = 0.22$ mm/s *vs.* $\Delta\delta_{\mathrm{HF}} = 0.60$ mm/s). The values obtained from the CCSD and B2-PLYP calculations are very close to one another. Therefore B2-PLYP is employed in the further calculations as a cost effective alternative to the coupled cluster method. Table 3 gives the contact densities and isomer shifts on iron in Fe^{II} and Fe^{III} oxidation

Table 3. ^{57}Fe electron contact densities and isomer shifts at different oxidation states incorporated in type I and type II clusters (see Fig. 1).

	Type I	Type II	$\Delta\rho$	$\Delta\delta$
Fe^{II}	15140.18	15139.98	-0.20	0.06
Fe^{III}	15140.89	15140.72	-0.18	0.05
$\Delta\rho$	-0.71	-0.74		
$\Delta\delta$	0.22	0.23		

states, for two different distribution patterns of Rb around Fe (see Fig. 1). In both types of Rb distribution patterns, change in the oxidation state of iron leads to a large variation of the isomer shift, of the order of $\Delta\delta$ (Fe^{II} - Fe^{III}) ~ 0.2 mm/s. These large variations in δ of iron sites with iron in Fe^{II} and Fe^{III} oxidation states agree qualitatively with the experimentally observed variations of the isomer shift in HT and LT phases. Thus, it can be concluded that iron in the HT phase is present predominantly in the form of Fe^{III}, whereas in the LT phase it is in the form of Fe^{II}.

Changing the distribution pattern of Rb^{I} ions (see Fig. 1) leads to much smaller variations of the isomer shift for both oxidation states of iron (see Table 3). The $\Delta\delta$ values reported in the last

column of Table 3 are consistent with the isomer shift differences of $\Delta\delta_{\mathrm{HT}} = 0.012$ mm/s and $\Delta\delta_{\mathrm{LT}} = 0.034$ mm/s observed for different iron sites within the HT phase and the LT phase respectively (see Table 1). Thus, these differences can be interpreted as originating from differences in the $\mathrm{Rb^{I}}$ ions distribution patterns around the $\mathrm{Fe^{III}}$ sites in the HT phase and around the $\mathrm{Fe^{II}}$ sites in the LT phase.

In the calculations reported above, it was assumed that the geometry of the coordination sphere of iron ions is the same in the HT and in the LT phases. In the HT phase, crystal structure of which is known experimentally, the $\mathrm{Fe^{III}}$ ions are surrounded by six cyano ligands at a distance $\mathrm{R_{Fe-C}} = 1.929$ Å. Because changing the oxidation state of iron to $\mathrm{Fe^{II}}$ should lead to contraction of the Fe-C bond length [17, 18], we have studied the effect of the bond length contraction on the contact densities and isomer shifts. In this study it was found that the bond length contraction in $\mathrm{Fe^{II}}$ coordination sites leads to a decrease in the isomer shift difference. Therefore, the value of $\Delta\delta(\mathrm{Fe^{II}} - \mathrm{Fe^{III}}) = 0.22$ mm/s obtained for the type I coordination at the HT experimental geometry should be corrected to a lower value (*e. g.* $\Delta\delta \approx 0.09$ mm/s for $\mathrm{Fe^{II}} - \mathrm{C}$ bond length of 1.89 Å), thus improving the agreement with the experiment (see Table 1) [3].

4. Conclusion

The origin of the different iron sites observed experimentally in the ^{57}Fe Mössbauer spectra of Prussian blue analogue $\mathrm{RbMn[Fe(CN)_6]\cdot H_2O}$ is analyzed with the help of theoretical calculations of the isomer shift on ^{57}Fe. In these calculations, a new formalism in which the isomer shift is treated as a response of the total electronic energy with respect to the variation of the nuclear charge radius (see Eq. (1)) is employed [12, 13, 14]. The relativistic calculations have been carried out at different levels of description of electron correlation varying from the Hartree-Fock method to the coupled cluster method (CCSD) and to the double hybrid density functional method (B2-PLYP) of Grimme[5].

The theoretically obtained ^{57}Fe isomer shift values enable one to interpret the experimentally observed $\Delta\delta_{\mathrm{HT-LT}}$ isomer shift differences (*ca.* 0.1 mm/s, see Table 1) between the HT phase and the LT phase of the $\mathrm{RbMn[Fe(CN)_6]\cdot H_2O}$ compound as originating from the change of the oxidation state of iron from $\mathrm{Fe^{III}}$ to $\mathrm{Fe^{II}}$. Two different iron sites observed within the HT and LT phases separately, which lead to $\Delta\delta$ values of the order of 0.01-0.03 mm/s (see Table 1), can be interpreted as originating from different distribution patterns of the $\mathrm{Rb^{I}}$ ions around the iron sites as shown in Fig. 1. The theoretical calculations yield the $\Delta\delta$ values of the order of 0.05 mm/s for the two types of $\mathrm{Rb^{I}}$ coordination thus corroborating the analysis of the experimental measurements presented by Vertelman *et al.* [3].

References

[1] Sato O, Iyoda T, Fujishima A and Hashimoto K 1996 *Science* **272** 704.
[2] Tokoro H, Ohkoshi S -L and Hashimoto K 2003 *Appl. Phys. Lett.* **82** 1245.
[3] Vertelman E J M, Lummen T T A, Meetsma A, Bouwkamp M W, Molnar G, van Loosdrecht P H M and van Koningsbruggen P J 2008 *Chem. Mater.* **20** 1236-38.
[4] Bartlett R J and Musial M 2007 *Rev. Mod. Phys.* **79** 291-352 and references cited therein.
[5] Grimme S 2006 *J. Chem. Phys.* **124** 034108.
[6] Ahlrichs R and May K *Phys. Chem. Chem. Phys.* **2000**, *2*, 943.
[7] Petersson G A and Al-Laham M A 1991 *J. Chem. Phys.* **94** 6081-90 and references cited therein.
[8] Fuentealba P, von Szentpaly L, Preuss H and Stoll H 1985 *J. Phys. B: At. Mol. Phys.* **18**, 1287.
[9] a) Dyall K G 2001 *J. Chem. Phys.* **115** 9136-43 b) Dyall K G 2002 *J. Comput. Chem. 23* 786-93.
[10] Dyall K G 1997 *J. Chem. Phys.* **106** 9618-26.
[11] Filatov M and Dyall K G 2007 *Theor. Chem. Acc.* **117** 333-38.
[12] Filatov M 2007 *J. Chem. Phys.* **127** 084101.
[13] Kurian R and Filatov M 2008 *J. Chem. Theory. Comput.* **4** 278-85.
[14] Kurian R and Filatov M 2009 *J. Chem. Phys.* **130** 124121.
[15] Filatov M and Kurian R *(manuscript in preparation).*
[16] a) Visscher L and Dyall KG 1997 *At. Data Nuc. Data Tables* **67**, 207. b) Visser O, Aerts PJ C, Hegarty D and Nieuwpoort W C 1987 *Chem. Phys. Lett.* **134**, 34-38.
[17] Neese F 2002 *Inorg. Chim. Acta* **337** 181-92.
[18] Nieuwpoort W C, Post D and van Duijnen P Th 1978 *Phys. Rev. B* **17** 91-98.